AN ABSTRACT OF THE THESIS OF

Jessica Anne Blank for the degree of Honors Baccalaureate of Science in Bioengineering presented on November 28, 2016. Title: Multiple Approaches to Novel Rifamycin Analogs to Combat MDR-TB.

Abstract approved:

_____

Taifo Mahmud

_____

According to the Center for Disease Control and Prevention (CDC), in 2015 10.4 million people worldwide became infected with tuberculosis (TB) with 1.8 million TB related deaths. Tuberculosis is a bacterial infectious disease caused by *Mycobacterium tuberculosis*, a slow growing yet highly infectious bacterium. Among the first line of treatments for TB is the antibiotic rifampin, a synthetic derivative of the natural product rifamycin B. Rifampin selectively inhibits bacterial RNA polymerase by binding to its β-subunit, effectively inhibiting protein synthesis leading to cell death. However, recently the development of multidrug resistant (MDR) and extensively drug resistant (XDR) TB has reduced the effectiveness of commercially available treatments, including rifampin. Bacterial resistance to rifampin is mainly due to mutations in the target protein RNA polymerase. Through a separate bio-computational modeling study, it was hypothesized that making a slight change to the rifamycin backbone may lead to a novel rifamycin analog that more effectively binds and inhibits mutated RNA polymerase. The suggested change, based on the bio-computational modeling study, is the removal of the methyl on C-7, lessening molecular steric hindrance. Methods focused initially on the genetic re-engineering of the bacterial producer of rifamycin, *Amycolatopsis mediterranei* S699, through the modification of the biosynthetic machinery. This can be achieved by

replacing the acyltransferase (AT) domain of module 1 of the *rif*-PKS (which recognizes methylmalonyl-CoA as the substrate) with the AT domain of module 2 of the *rapamycin* PKS (which recognizes malonyl-CoA) using a double crossover homologous recombination. However, there were some issues in the transformation of the final construct into the competent *A. mediterranei* cells leading to the exploration of another approach. By observation, it was recognized that old plates of *Amycolatopsis mediterranei* S699 began to show evidence of different metabolites, one of which resembled, in mass spectrometry measurements, that of a desmethylrifamycin SV. In order to test this, cells were starved on different media and then tested at various points in time for metabolite production. After analysis, the compound of interest was identified to be 12-desmethylrifamycin SV. This compound did show significant activity against *M. tuberculosis,* but not against drug resistant forms. The selective removal of the methyl group on C-12 is most likely due to enzyme catalysis. There are two genes, which encode cytochrome P450 monooxygenases (*rif-orf13* and *rif-orf16*), within the rifamycin biosynthetic gene cluster that may be responsible for the oxidation and removal of the methyl group. Therefore, both of them were cloned and heterologously expressed in *Escherichia coli*. However, the proteins were found to be insoluble. Therefore, detailed investigations of these proteins cannot be done at this point in time, and will have to wait until soluble proteins are available. Future work would include refinement of the heterologous expression methodology and full characterization of Orf13 and Orf16 to determine their involvement in the formation of 12-desmethylrifamycin SV.

Corresponding email address: jessicaanneblank@gmail.com

Multiple Approaches to Novel Rifamycin Analogs to Combat MDR-TB

By

Jessica Anne Blank

A PROJECT

Submitted to

Oregon State University

Honors College

in partial fulfillment of
the requirements for the
degree of

Honors Baccalaureate of Science in Bioengineering
(Honors Scholar)

Presented November 28, 2016
Commencement June 17, 2017

ACKNOWLEDGEMENTS

Table of Contents

CHAPTER 1

INTRODUCTION

1.1. The History and Socioeconomic Impact of Tuberculosis

Tuberculosis (TB) is a well known and often thought of disease within the landscape of global medicine and pharmacological research. The presence of TB is not a new entity on the medical market, there is current evidence to suggest that modern strains of the bacteria causing TB, *Mycobacterium tuberculosis* (Figure 1)*,* originated 15,000-20,000 years ago.[1] East Africa is thought to be the originating location of TB with many early progenitors of *M. tuberculosis* existing over three million years ago.[1] Often referred to as 'consumption' in European literature, Tuberculosis has led an important role in the history of humankind as well as infectious disease research. After the successful staining and visualization of the bacteria causing TB by Robert Koch in 1882, the real battle against the deadly disease began.[2]
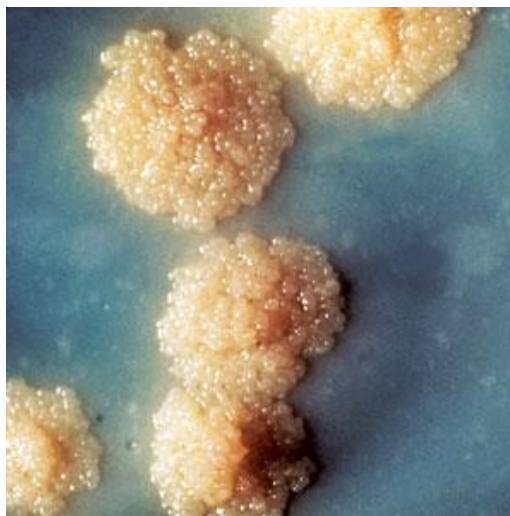
Figure 1: M. tuberculosis culture showing colony morphology.[3]

Initial treatment methods generally involved patient isolation, proper nutrition, and in some cases, intentional lung capacity reduction. It was not until 1944 that the first drug, streptomycin, was deemed effective against *M. tuberculosis* with rifamycins coming into use in 1957.[1] As a result of the boom in antibacterial drugs used against *M. tuberculosis*, there has also been a boom in the prevalence of multi-drug resistant tuberculosis (MDR-TB). According to the Center for Disease Control and Prevention (CDC) the emergence of MDR-TB is a result of many factors including but not limited to: failure to complete the drug regimen, failure to complete the drug regimen correctly, and development of TB after taking TB medication previously.[4] Although there is a great deal of research going into the eradication of tuberculosis, there was a reported 10.4 million new cases of TB and 1.8 million deaths related to TB in 2015 alone.[5] Furthermore, over 480,000 people developed MDR-TB globally in 2014, with most cases appearing in India, China, and Russia.[6] TB is further complicated by the presence of other dangerous diseases such as HIV with TB being the number one killer among HIV infected patients.[5]

When looking at disease, it is important to not only talk about the disease itself but also the cultural and socioeconomic impact of the disease on communities and individuals. A study published in 1999 in regards to families in India showed a total of 83 workdays lost to TB per person per year with 15 % of women facing social rejection and 11 % of children discontinuing their school studies.[7] According to the World Health Organization, 20-30 % of household income can be lost when a family member develops TB. The global economic burden of TB, based on household income lost, equals approximately one billion dollars a year.[8] Morris et al. (2014) performed qualitative

interviews of MDR-TB patients in Mexico and discovered that many individuals lost a sense of personal identity because of their lack of ability to participate in work and play as well as the stigma associated with their condition.[9] In general, many individuals experience some form of social and economic (69 % and 30.3 %, respectively) impact with tuberculosis infections, causing a severe shift in the quality of life outside of the physical impact of the disease.[10]

1.2. The History of Antibiotics

Infectious diseases are not new to the world. They have ravaged every continent to varying degrees, killing off populations of people and causing widespread panic. Although these diseases were recognized as dangerous and symptoms were documented, it was not until the 19th century that causation between microscopic pathogens and infectious disease was noted.[11] During that same time period, diseases such as diphtheria, diarrhea, pneumonia, as well as tuberculosis were the number one killers of children and adults.[11] Sanitation was a large contributor to the prevalence of these diseases, it was, however, obvious that other, more direct treatments were going to be necessary to eradicate or at least significantly reduce fatality and spreading. Although the conscious use of antibiotics did not begin until the 1900's, the use of natural products for the treatment of diseases dates back to the time of the Romans where there is evidence of diet-obtained tetracycline in the bones of people.[12] There is also anecdotal evidence that the soils of Jordan were used to prevent skin infections. This soil, it turns out, contains actinomycete bacteria that produces actinomycin antibiotics. The use of this soil is still done today as an inexpensive alternative to pharmaceutical drugs.[12]

Paul Ehrlich is often associated with the introduction of the antibiotic era. He set out to find a 'magic bullet' drug that would be able to selectively target pathogens and leave the host organism with minimal side effects and damage. In the process of finding this magic drug, he first focused on syphilis. Along with colleagues, he worked to develop safer derivatives of Atoxyl, a highly toxic drug.[12] He developed a screening process that eventually became the cornerstone of drug development while developing the successful Salvarsan anti-syphilis treatment.[12] There is no short list of some of the great discoveries in antimicrobial chemotherapy, from Ehrlich to Fleming, from Prontosil to the new drugs being discovered today. Although the world continues to increase sanitation and improve the prevention of disease through vaccines, there will always be a need for antimicrobial agents as microbes mutate.

1.3. The History of Anti-Tuberculosis Drugs and the Treatment of TB

The first drug that showed antimicrobial activity towards *M. tuberculosis* was streptomycin in 1944, followed by rifamycins in 1957.[1] Rifampin is a semi-synthetic derivative of rifamycin B, a polyketide antibiotic produced by the bacterium *Amycolatopsis mediterranei*. In the development of anti-TB drugs, rifamycin B underwent many structural alterations in order to find a highly active agent against tuberculosis. One of the most active derivatives is what is known as rifampin (Figure 2), the most common drug used today to fight TB infections.[13] After success in clinical trials, rifampin was put into use in 1968.
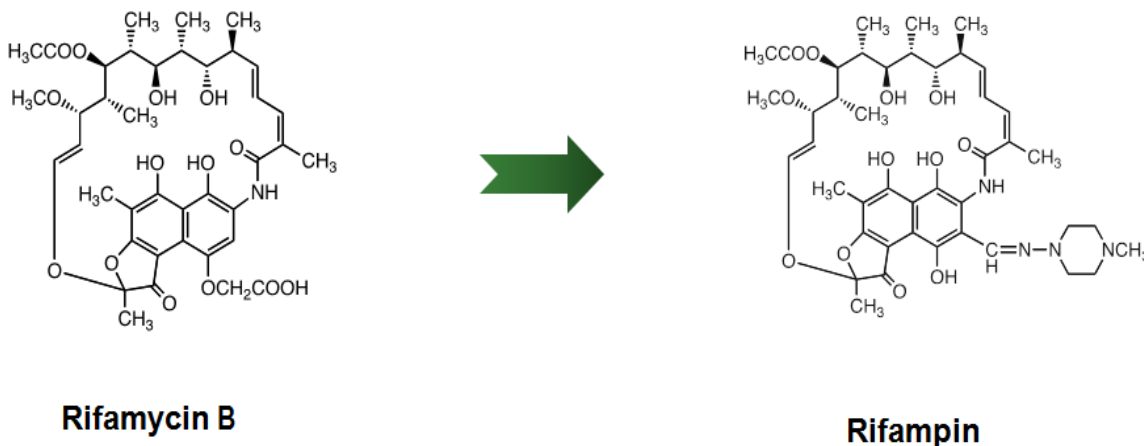
Figure 2: The difference in structure of rifamycin B and rifampin.

There are many treatment plans for TB infected patients. These regimens include a 2-month intensive phase along with a 4- or 7-month continuation phase.[14] The intensive phase involves the use of isoniazid, rifampin, ethambutol, and pyrazinamide whereas the continuation phase involves using just isoniazid and rifampin. These drugs are considered first-line drugs for the treatment of TB. There are also many second-line drugs that can be used but often these drugs are more difficult to obtain, are expensive, and can cause significantly more dangerous side effects with their higher toxicity.[15] These drugs include fluoroquinolones, aminoglycosides (kanamycin, capreomycin), ethionamide/prothionamide, p-amino salicylic acid, and cycloserine.

1.4. Rifamycin B Biosynthesis

The assembly of the rifamycin linear polyketide backbone is catalyzed by a set of proteins called polyketide synthases (RifA-RifE) using 3-amino-5-hydroxybenzoic acid (AHBA) as a starter unit, and two acetates and eight propionates as extender units.[16]

Subsequently, the amide synthase RifF catalyzes the cyclization of the polyketide structure and its release from the polyketide synthase. Each module within the polyketide synthase proteins contains a number of domains that play different roles in the process of polyketide chain elongation. Figure 3 illustrates the biosynthetic process of the rifamycin polyketide starting with AHBA. It also shows genes that encode putative regulatory and tailoring proteins involved in biosynthesis.
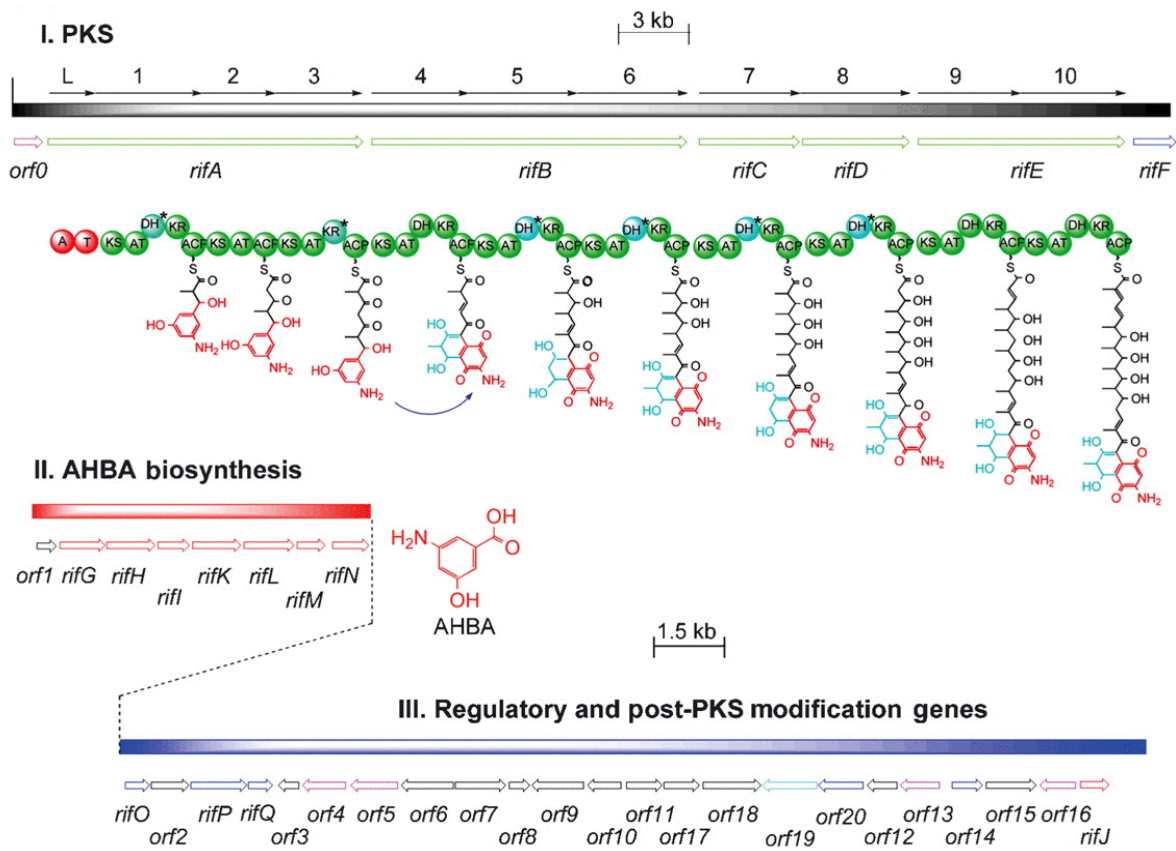
Figure 3: Genetic organization and biosynthesis of rifamycin B.[23]

1.5. Rifampin's Mechanism of Action

Rifampin's mechanism of action is what makes it such as potent and useful antibacterial agent. Rifampin selectively targets bacterial RNA polymerase (RNAP). This selective targeting prevents the drug from also affecting host cell populations, reducing side effects and host damage. It binds deep in the β subunit of RNAP, within the DNA/RNA channel, 12Å away from the active site. By binding to the β subunit, it effectively blocks the path for the elongating mRNA strand, preventing the strand from going beyond 2-3 nucleotides.[17] The inability to produce mRNA subsequently prevents the production of protein, leading to cellular death. The presence of rifampin resistant tuberculosis has now complicated the TB treatment protocol. The cause of this resistance is mutations in the region that encodes the β subunit of RNAP. This region is 81 base pairs and 96% of rifampin-resistant strains of *M. tuberculosis* have mutations in this region.[18] The most common mutation is the S531L mutation where a serine at amino acid 531 is replaced with a leucine. This replacement increases steric hindrance between the methyls on leucine and the methyl at C-7. These mutations prevent the deep binding of the β subunit by rifampin, allowing the elongation of mRNA by RNAP and resulting in proliferation of the bacteria.

1.6. Techniques

The following general techniques were employed throughout experimentation and were appropriately modified according to the experimental aims. All specifics are fleshed out in the experimental section and are noted as such.

1.6.1. Culture

Solid culture plating was used to grow and isolate colonies for further experimentation. Various media recipes (including differing antibiotics) were used throughout experimentation. All culture broth was autoclaved prior to use to ensure sterility. Plating of bacteria was done in a sterile hood with sterile equipment. The plates were put into an incubator at the needed temperature for growth and left for a specific time frame to ensure proper growth without introducing contamination or overgrowth. Colonies were isolated and placed in liquid culture tubes for further growth under incubation.

1.6.2. Plasmid Isolation

Plasmid isolation was based on the QIAprep Spin Miniprep kit (Qiagen) but without the column. Three solutions were made for isolation:

P1: 6.1 g/L Tris, 3.7 g/L EDTA-2H_2O, pH to 8.0 with HCl, 100 mg/L RNAse A, Store at 4 °C

P2: 8g/L NaOH, 100 mL/ L 10% SDS, Store at room temperature

P3: 588g/L potassium acetate, pH to 5.5 with Acetic acid, store at room temperature

To start the procedure of plasmid isolation, 1.5 mL of liquid culture was added to an eppendorf tube and spun at 16000g for 2 minutes to pellet cells. The supernatant was decanted and this was repeated up to two times if desired to pellet more cells. The cells were resuspended in 250 µl of P1 (250 µl per 5 mL of cell culture used). No cell clumps were visible. Another 250 µl of P2 (250 µl per 5 mL of cell culture used) was added and

the tube was inverted 6 times. No vortexing was used at this step. The solution was viscous and slightly clear but the lysis was not allowed to go beyond five minutes. At this point, 350 µl of P3 was added (350 µl per 5 mL of cell culture used) and the tube was inverted 6 times immediately allowing the solution to become cloudy. The tube was then centrifuged for 10 minutes at 16000g and 700 µl of the supernatant was transferred to a tube with 700 µl of isopropanol and put on ice for 15 minutes. The tube was centrifuged for 30 minutes at 16000g to pellet the plasmid DNA. After centrifugation, the supernatant was removed and 300 µl of 70% ethanol was added and the tube was centrifuged for 10 minutes at 16000g. The ethanol was removed by decanting and the pellet was dried via a speedvac for 20 minutes. When desired, the pellet was resuspended in a desired volume of sterile ddH$_2$O and kept at 4 °C.

1.6.3. Genomic DNA Extraction

Genomic DNA extraction was used to prepare DNA as a template for PCR in fragment amplification from primers. Scraped cells were put into 200 µl STE buffer and 10 µl of lysozyme and incubated for 1 hour at 37 °C. After the incubation, 200 µl of 2.5 % SDS was added followed by 10 µl proteinase K and incubated at 57 °C for two hours. An equal volume (400 µl) of phenol and chloroform was added and mixed vigorously. This mixture was centrifuged for 10 minutes at 13000 rpm. The aqueous layer (top layer) was removed and put into a separate tube. This was the genomic DNA. At this point, 100 µl of 1.5 M sodium acetate and 500 µl 100 % cold ethanol was added and the mixture was left at -20 °C for 10 minutes. The mix was then centrifuged for 10 minutes at 13000 rpm and the ethanol was discarded and 500 µl of 70 % ethanol was added. Again, the mix

was centrifuged for 10 minutes at 13000 rpm. The supernatant was discarded and the genomic DNA was dried on a speed vac until no ethanol remained.

1.6.4. PCR

Polymerase chain reaction (PCR) was used to amplify a few copies of DNA across several orders of magnitude. The ingredients, dd H_2O, buffer, $MgSO_4$, dNTP, primers, template DNA, and DNA polymerase, were mixed. The PCR was run through the desired thermal cycle. The results were then analyzed using gel electrophoresis.

1.6.5. Restriction Endonucleases

Restriction enzymes were used to cut the plasmid DNA at specific spots for DNA insertion and subsequent incorporation into the bacterial plasmid DNA. The following steps can be applied to many general restriction enzymes. The plasmid, restriction enzyme(s), and buffer were mixed together and incubated for one hour (or less if a fast digest enzyme) at 37 °C. After incubation, the reactions were heat inactivated for 20 minutes at 65 °C.

1.6.6. Electrocompetent Cells

Electrocompetent cells were used for transformation of plasmids and subsequent growth and multiplication of cells with plasmids. Making electrocompetent cells requires that all components be ice cold when in use. To begin, glycerol stocks of cells must be streaked on a plate and incubated overnight at 37 °C. The next day, a colony was selected and a 10 mL liquid culture was started and put on a shaker overnight at 37 °C. On the third day, 1 L LB medium was inoculated with the 10 mL starter culture and grown on a

37 °C shaker until the OD_{600} was 0.35-0.4. Once it reached this range, the flask was immediately put on ice to stop growth. The cells were then put through multiple spin cycles, condensing the cells into fewer and few bottles and eventually putting the cells into a glycerol solution. Aliquots were then flash frozen and stored at -80 °C.

1.6.7. Dephosphorylation

Dephosphorylation was performed prior to ligation. It involved mixing DNA, shrimp phosphatase, and buffer and then incubating for one hour at 37 °C. After incubation, the reaction was heat inactivated for 30 minutes at 65 °C.

1.6.8. Ligation

Ligation allowed for the insertion of a DNA fragment into an enzymatically cut plasmid. The ingredients: cut plasmid, DNA fragment, ATP, ligase, buffer, and ddH_2O, were mixed and then incubated at 16 °C overnight (28 °C for two hours was also sufficient).

1.6.9. Transformation for Electrocompetent Cells

Transformation involved the use of competent cells for the insertion of DNA, in this case in the form of a plasmid, into said cells. The competent cells were thawed on ice before cold DNA was added. After sitting for one minute on ice the mixture was transferred to a cold 1 mm electroporation cuvette and pulsed at 2.49 volts. After the pulse, 1 mL of SOC media was added to the cuvette, mixed, and then put into a microcentrifuge tube. The tube was then incubated at 37 °C for 60 minutes.

Transformations were plated on antibiotic selective plates and incubated at 37 °C overnight.

1.6.10. Gel Electrophoresis

Gel electrophoresis was used to separate DNA based on size, with the largest pieces moving the least down the gel. The agarose gel was poured into the mold and allowed to solidify. The loading buffer was added to each sample and mixed well. A ladder was needed in one of the wells and then the samples were added, keeping track of which lane each sample went into. The gel was run until the dye front reached three quarters of the way down the gel.

1.6.11. Mass Spectrometry

To prepare samples for mass spectrometry, small cubes (1cm x 1cm x 1cm) of cells and solid medium were placed in microcentrifuge tubes with 100 % methanol. The tubes were centrifuged to remove any particulates and the liquid was removed for analysis. These tubes were then analyzed with liquid chromatography mass spectrometry (LC-MS). The samples were run on negative mode which is common for molecules containing carboxyl groups and phenolic hydroxyl groups.

1.6.12. Metabolite Extraction

Extraction involved the removal of the metabolites produced by the cells present on plates. The solid agar plate was cut up into smaller cubes and put into a 500 mL flask. Methanol was poured into the flask until the methanol just covered the chunks, allowing for full submersion. The cubes were allowed to soak for three hours and extraction liquid

(methanol and any metabolites) were then put into 50 mL falcon tubes and centrifuged for 20 minutes at 3400 rpm. A rotovap was then used to evaporate the methanol from the sample. Vials were weighed before and after the dry sample was added to obtain a total mass of the sample.

1.6.13. Chemically Competent Cells

The cells were centrifuged at 2800 rpm for 15 minutes at 4 °C and then 10 mL of $CaCl_2$ was added and again the cells were centrifuged as before. The supernatant was removed and the cells were resuspended in 2.5 mL $CaCl_2$. Aliquots of cells were flash frozen and stored at -80 °C.

1.6.14. Heat Shock Transformation of Chemically Competent Cells

To transform chemically competent cells, DNA was added to the cells on ice and was left to sit for 20 minutes. The mixture was shocked in a 42 °C water bath for 30 seconds and put immediately on ice for 2 minutes. LB media was added and then the mixture was put in a 15 mL tube and shaken at 37 °C for 45 minutes.

1.6.15. Protein Expression

The starter culture was prepared by inoculating the media with the appropriate antibiotic and one colony. The culture was shaken at 37°C for 6 hours. This starter culture was used to inoculate a larger culture. This larger culture was shaken at 30 °C for 3 hours. When the culture reached an OD_{600} of 0.4 the flasks were put into the 18 °C shaker and allowed to reach 18 °C. At this point, δ-amino-levulinic acid (0.5 mM) was

added and shaken for 20 minutes before an inducer (IPTG, 100 μM) was added. The culture was shaken overnight at 18 °C.

1.6.16. SDS-PAGE

A SDS-PAGE was used to separate proteins by size. The gel and the samples were prepared before running at 60V for 45 minutes. At this point, the voltage was raised to 100V for 2 hours, until the dye front reached the bottom. Methylene blue dye was added for one hour and then removed using destaining buffer (100 mL acetic acid, 300 mL methanol, and 100 mL ddH$_2$O) for one hour or more until most residual stain was removed.

1.6.17. Agilent HF Bond Elute C18

Samples were initially purified using a C18 cartridge filled with a silica-based stationary phase. The sample was mixed with celite and allowed to form a crumbly paste. The paste was dried and then loaded into the C18 cartridges with a silica stationary phase. A vacuum was attached and fractions were loaded and collected.

1.6.18. HPLC

High performance liquid chromatography (HPLC) was used for purification of samples for later testing. The sample was pumped within a mobile phase at high pressure through a column with a stationary phase.

CHAPTER 2

POLYKETIDE BACKBONE MODIFICATION

2.1. Introduction

The previous experimental success by Nigam et al. (2014) in which modification of the rifamycin polyketide synthase (PKS) responsible for the production of rifamycin B was the basis for the following experimentation. In this previous study, the acyltransferase (AT) domain of module 6 of the rifamycin PKS in *Amycolatopsis mediterranei* S699 was replaced with that of module 2 of the rapamycin PKS via a double crossover recombination. The recombinant strain produced a novel compound, 24-desmethylrifamycin B, which lacks a methyl group at C-24 of the polyketide backbone. 24-Desmethylrifamycin B was then converted to 24-desmethylrifampin by synthetic modifications and the product showed excellent antibiotic activity.[19] Following the basic steps outlined in this study, the goal became to modify the rifamycin PKS by replacing the AT domain of module 1 with the AT domain of module 2 of the rapamycin PKS (Figures 4). This will be achieved by a double crossover recombination procedure as shown in Figure 5. The mutant should, hypothetically, produce a 7-desmethylrifamycin analog (Figure 6), which may be further modified chemically to give 7-desmethylrifampin.
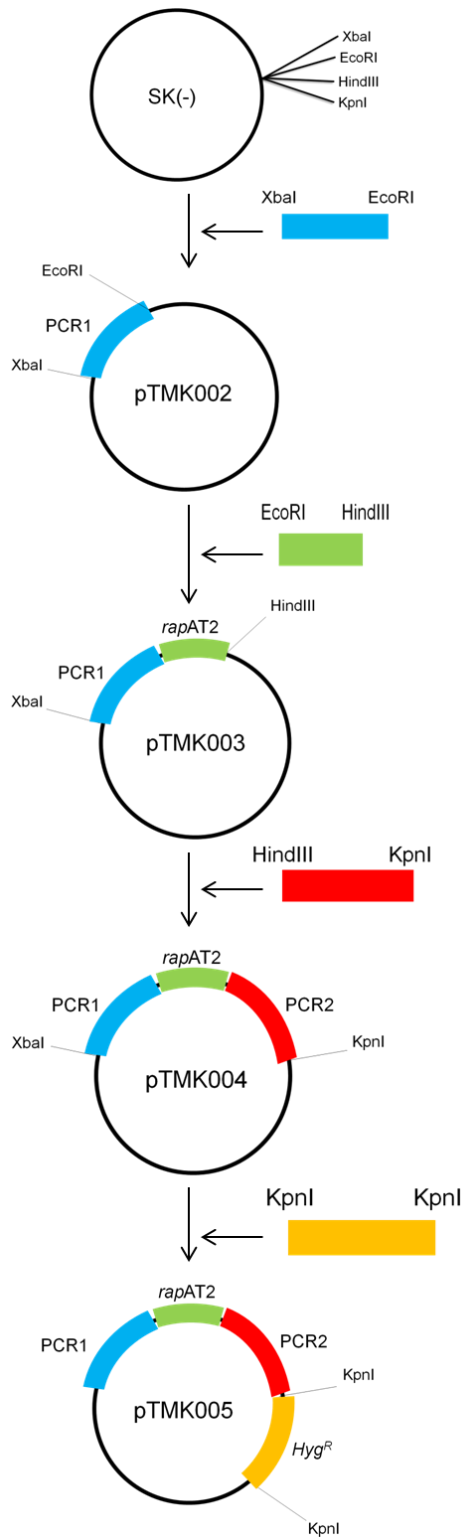
Figure 4: Plasmid construction using the SK (-) vector and DNA fragments isolated using PCR. Restriction enzyme sites are shown as well as the final antibiotic resistant Hyg insert.
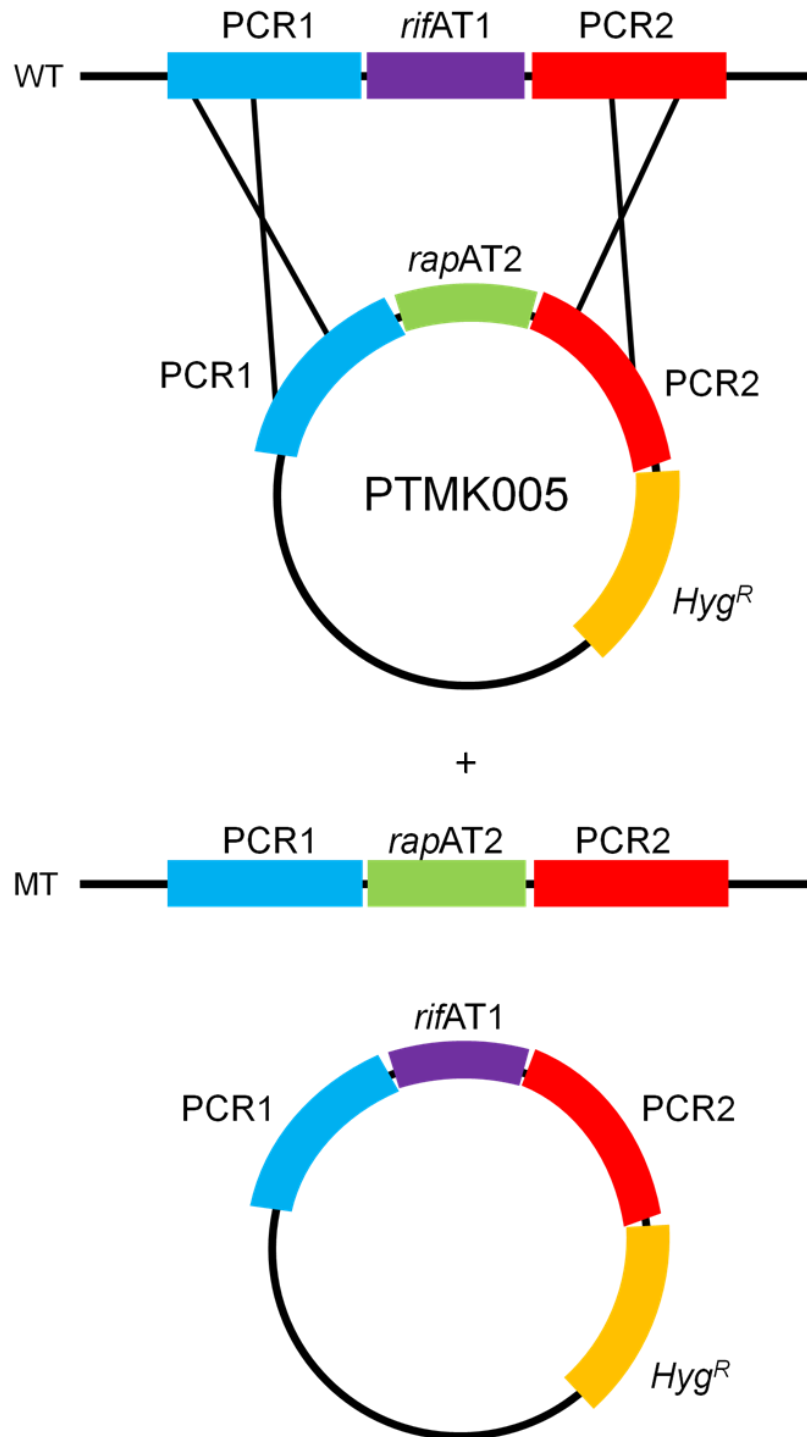
Figure 5: Schematic overview of the double crossover homologous recombination events predicted to occur to produce the AT1 mutant.
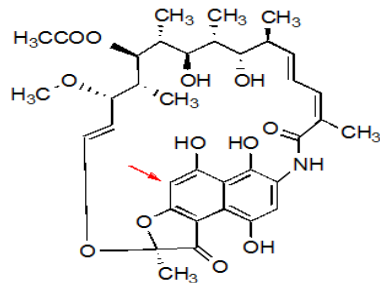
Figure 6: 7-Desmethylrifamycin SV is the target molecule with possible reduced steric hindrance and improved antibiotic activity against MDR-TB.

2.3. Experimental Procedures

2.3.1. Bacterial Strains, Plasmids, and Culture Media

The producer of rifamycin B, *A. mediterranei S699* (wild type), was grown at 30 °C on YMG agar plates (4 g/L yeast, 10 g/L malt extract, 4 g/L glucose, and 15 g/L agar, pH 7.2-7.4). pBluescript SK(-) was used as the vector for domain replacement and *E. Coli* DH10β cells were used for the propagation and isolation of plasmids.

2.3.2. Construction of pTMK005

For the construction of the pTMK005 replacement cassette, AT1-flanking regions were engineered upstream and downstream of AT1. A 1.6–kb DNA fragment upstream of AT1 was engineered around the ketosynthase enzyme and with XbaI and EcoR1 restriction sites. The forward primer was 5'-*CTCTAGA*GAGCCGATCGCGATCGTGGGGATGGCC-3' and the reverse primer was 5'-*CGAATTC*CTCACGGCCCATCCCGGCCCACTG-3'. A 1.45-kb DNA fragment

downstream of AT1 was engineered around the dehydratase enzyme and with HindIII and KpnI restriction sites. The forward primer was 5'-*CAAGCTT*TGGGTCGACTTGCCGACCTAC-3' and the reverse primer was 5'-*CGGTACC*GGTGAGCTCGTCCAGGAG-3'. These fragments were obtained by PCR amplification using *A. mediterrainei* S699 as template DNA. *rap*AT2 was obtained from the AT6 mutant using primers 5'-CC*GAATTC*TTCCCGGGTCAGGGGTCGCAGCG and 5'- CCC*AAGCTT*ACCCAGCACCGCGGACCACTC, forward and reverse respectively.[19] The two amplicons, PCR1, *rap*AT2, and PCR2 were inserted into the pBluescript SK(-) vector in said order. SK(-) was digested with XbaI and EcoR1 and treated with shrimp alkaline phosphatase. The PCR1 insert was ligated into the vector making pTMK002. Next, the process was repeated with the *rap*AT2, a 0.85-kb fragment. The plasmid, pTMK002 was digested with EcoR1 and HindIII and *rap*AT2 was ligated into the vector making pTMK003. Finally, the PCR2 fragment was inserted by digesting pTMK003 with HindIII and KpnI and ligating the fragment into the plasmid making pTMK004. During each of these steps, each plasmid was electroporated into DH10β cells and colonies were selected after overnight growth on antibiotic (ampicillin) selective plates. The plasmid was cut once again at KpnI and a hygromycin resistance gene (1.7-kb) was inserted for later plate selection during the final transformation. The final constructs are shown in Figure 7.
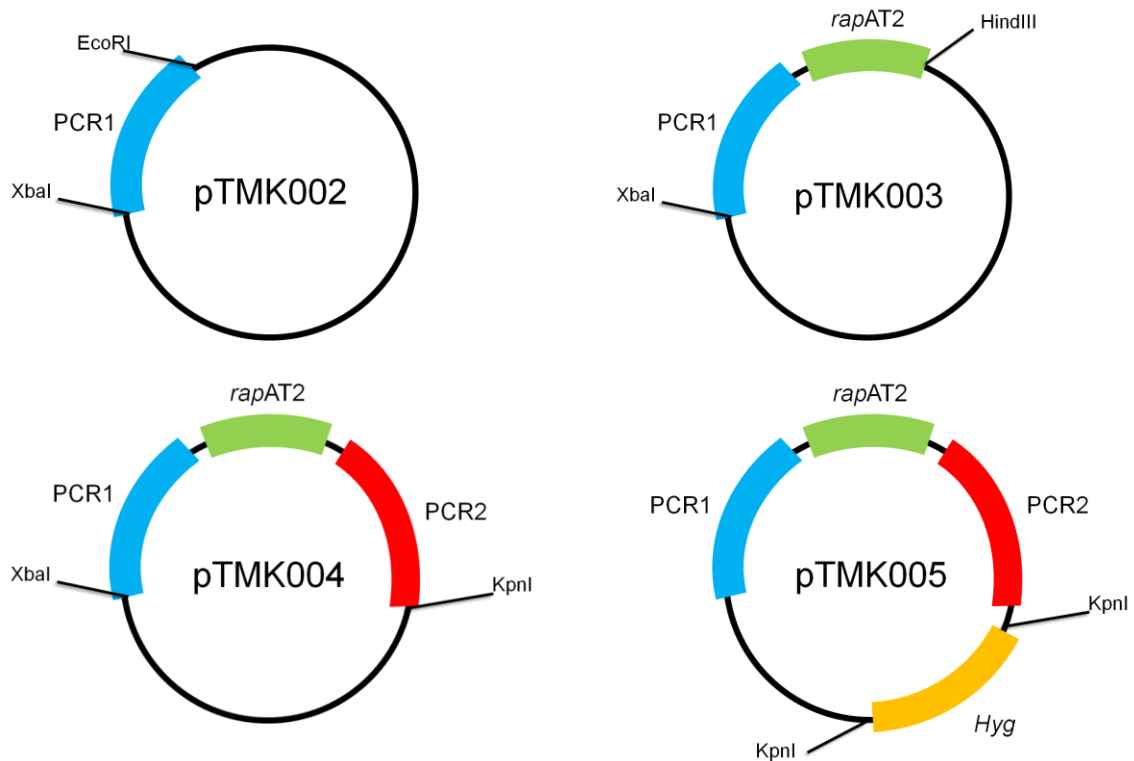
Figure 7: Final plasmids used throughout the construction of the replacement cassette.

2.3.3. Genetic Manipulation of *Amycolatopsis mediterranei* S699

Standard techniques were carried out for the routine genetic procedures of genomic DNA isolation, plasmid isolation, and restriction endonuclease digestion. The pTMK005 was isolated from *E. coli* DH10β cells and transformed to *E. coli* ET12567/pUZ8002 for later use. A preparation of *A. mediterranei* S699 competent cells and the transformation of heat-denatured pTMK005 into *A. mediterranei* S699 were carried out as in protocols described in literature.[20,21] The transformation mixture was overlaid on plates containing 70 μg/ ml Hygromycin B and the plates were incubated at 30 °C for 10-15 days.

2.4. Results and Discussion

2.4.1. Construction of the Replacement Cassette

The construction of pTMK005 replacement cassette took many steps and involved multiple rounds of ligations and electroporation. After the first insertion of PCR1 making the pTMK002 plasmid, the plasmid was checked using gel electrophoresis. Figure 8a shows the resultant gel using a double digestion with XbaI and EcoR1. The resultant bands are present at 3-kb which is SK(-) and 1.6-kb for the PCR1 insert. Figure 8b represents the double and single digestion after the addition of *rap*AT2 into the vector making pTMK003. The single digestion was with HindIII, providing the 5.45-kb band and the double digestion used XbaI and EcoR1 giving a 3.85-kb band for the SK(-) and *rap*AT2 and a 1.6-kb band for PCR1. Figure 8c represents the single digestion after the PCR2 insertion making the plasmid, pTMK004. The digestion was performed with HindIII giving a 6.9-kb band. Figure 8d is a single digestion after the insertion of the Hyg^R gene. The digestion with KpnI gives two bands, one for Hyg^R itself (1.7-kb) and one for the rest of the plasmid (6.9-kb).
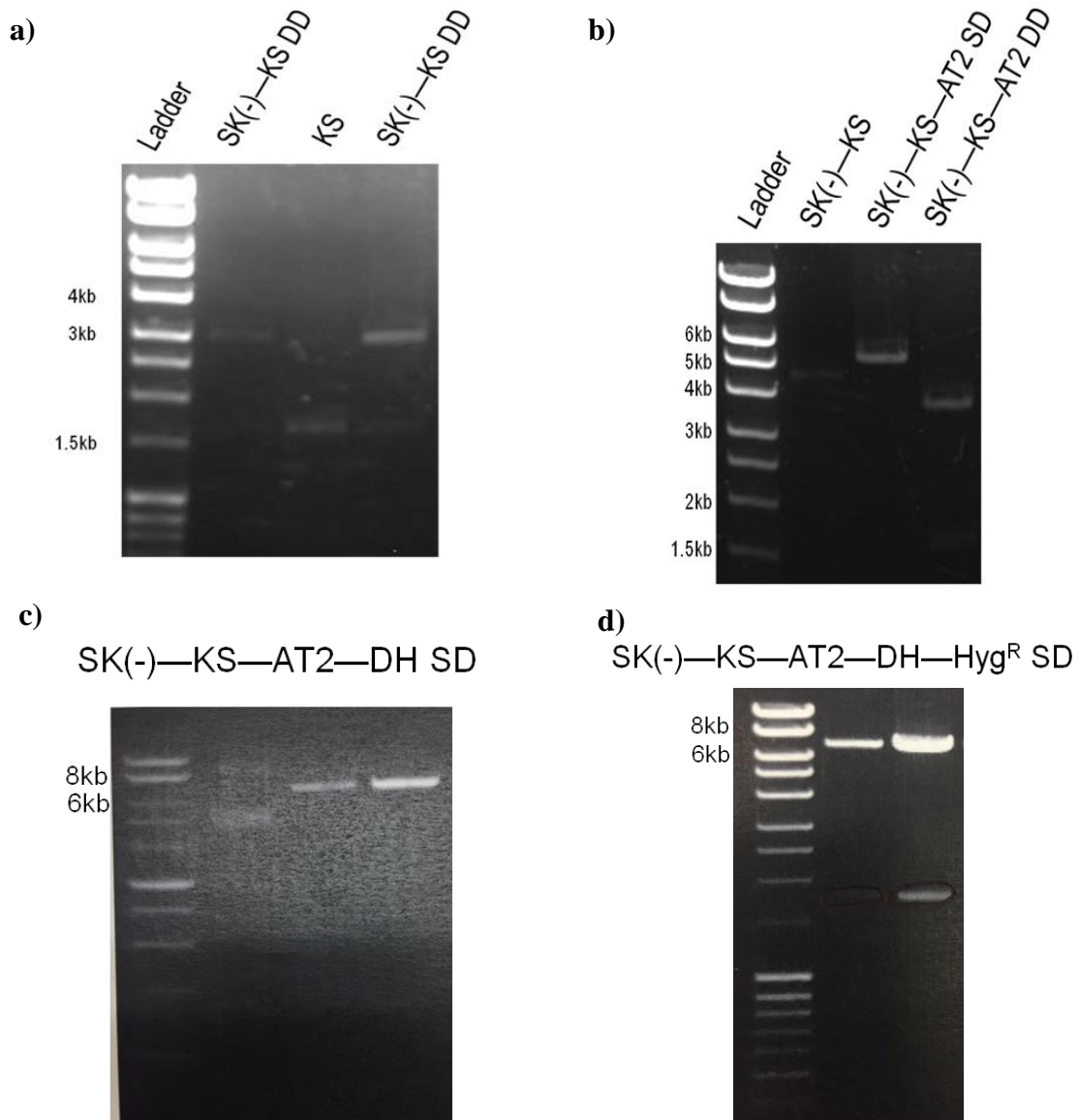
Figure 8: a) The double digestion (DD) of pTMK002 using XbaI and EcoR1. Bands present at 3-kb and 1.6-kb indicate proper insertion. b) The single (SD) and DD of pTMK003. The SD was with HindIII giving a 5.45-kb band. The DD was with XbaI and EcoR1 giving 1.6-kb and 3.85-kb bands. c) The SD (shown twice) of the pTMK004 with HindIII reveals a band at 6.9-kb. d) The SD of pTMK005 with KpnI, yielding two bands. One is at 1.7-kb which is the Hyg^R gene and the other is the rest of the plasmid (6.9-kb).

2.4.2. Transfer of pTMK005 into *A. mediterranei*

The transformation of *A. mediterranei* using pTMK005 presented problems. Electroporation was unsuccessful and the construct was unable to enter the bacteria. As a result, further experimentation and troubleshooting are necessary to determine why the electroporation was unsuccessful as well as how to increase success rates.

CHAPTER 3

Production of a Novel Rifamycin Analog by *Amycolatopsis Mediterranei* S699 after Extended Time of Cultivation

3.1. Introduction

As was stated previously, *Amycolatopsis mediterranei* S699 is the producer of rifamycin B. It was noted, however, that after a prolonged incubation, the strain began to produce a new rifamycin analog. This observation was based on the increased presence of a spike on the mass spectrometry (*m/z* 682 [M-H]⁻). This is consistent with what is expected of a desmethylrifamycin SV.[21] This phenomenon was only seen in older plates of *A. mediterranei* S699 and as a result, it was hypothesized that this peak represents the presence of a naturally occurring desmethyl analog of rifamycin. It was thought that this may be the desired 7-desmethylrifamycin SV and so it was further explored. Many methods to induce production of this metabolite were used, including growing the bacteria on different agar media and modifying the concentrations of the components of the media. The overall goal was to determine if this compound that is naturally produced is in fact the desired 7-desmethyl analog (Figure 4, section 2.1), and if so, what is the best way to induce its production.

3.3. Experimental Procedures

3.3.1. Plating of *Amycolatopsis mediterranei* S699 Cells on Various Media

Many medium compositions were explored including minimal medium (L-asparagine: 0.5 g/L, K_2HPO_4: 0.5 g/L, $MgSO_4$ $7H_2O$: 0.2 g/L, $FeSO_4$ $7H_2O$: 0.01 g/L, Glucose: 10 g/L, and ddH_2O) and different component concentrations of YMG media. Initially, four modified YMG medium (listed in Table 1) were tested in order to determine the best recipe for efficient production of the expected 7-desmethyl analog. These various forms of medium were selected to allow very little nutrients all the way to fully nutritious. More optimization of this media could be done in further testing. Cells were streaked across the surface of the solid media from a frozen glycerol stock covering as much of the surface as possible. The plates were allowed to grow for five days at 30 °C to obtain sufficient coverage.

Table 1: The four variations of YMG media utilized for extended cultivation.

Yeast (g/L)	Maltose Extract (g/L)	Glucose (g/L)	Agar (g/L)
4	10	0.5	3.75
1	2	0.5	3.75
2	5	0.25	3.75
2	5	0	3.75

3.3.2. Starvation of Cells

After ten days of growth at 30 °C, the plates were moved to a dark location and kept at room temperature. The bacteria on the plates were allowed to continue to produce metabolites and feed off the solid medium. They were left under these conditions for 35 days before they were checked on the mass spectrometer. They were then returned to the dark, room temperature conditions for an additional eleven days before further testing.

3.3.3. Testing Metabolite Composition

Mass spectrometry was used to analyze metabolite compositions in the agar samples. A small, 1 cm x 1 cm x 1 cm cube of agar was removed from the plate and put into a 1.5 mL microcentrifuge tube containing 1 mL of methanol. The agar sat in the methanol for an hour before being centrifuged. The samples were then analyzed using mass spectrometry (MS). They were run on a negative ion mode, which is common for molecules containing a carboxyl or a phenolic hydroxyl group.

3.3.4. C18 and HPLC Purification of Desmethylrifamycin SV

Samples were initially purified using a C18 cartridge filled with a silica-based stationary phase. The sample was mixed with celite and allowed to form a crumbly paste. The paste was dried and then loaded into the C18 cartridges with a silica stationary phase. A vacuum was attached and fractions were eluted with different solvent mixtures. 12-Desmethylrifamycin SV was purified by HPLC using a YMC column, 250 x 10 mm, acetonitrile-(0.005 M) ammonium formate gradient (40 % acetonitrile for 12 min, then 100 % acetonitrile for 25 min, then 40 % for 30 min), and a flow rate of 2 mL/min.

3.4. Results and Discussion

3.4.1. Mass Spectrometry Analysis of a 12-desmethylrifamycin SV

After initial realization that the observed product could be the 7-desmethylrifamycin SV, a tandem mass spectrometry was performed to determine the general location of the missing methyl. Figure 9 shows the tandem mass spectra of both rifamycin SV (Figure 9a) and the degradation product (Figure 9b). The molecular mass of a fragment containing the naphthalene ring structure of the degradation product (m/z 258) is 14 Da less than that of rifamycin SV (m/z 272), indicating that a methyl group is missing in the former fragment (either on C-7 or C-12).
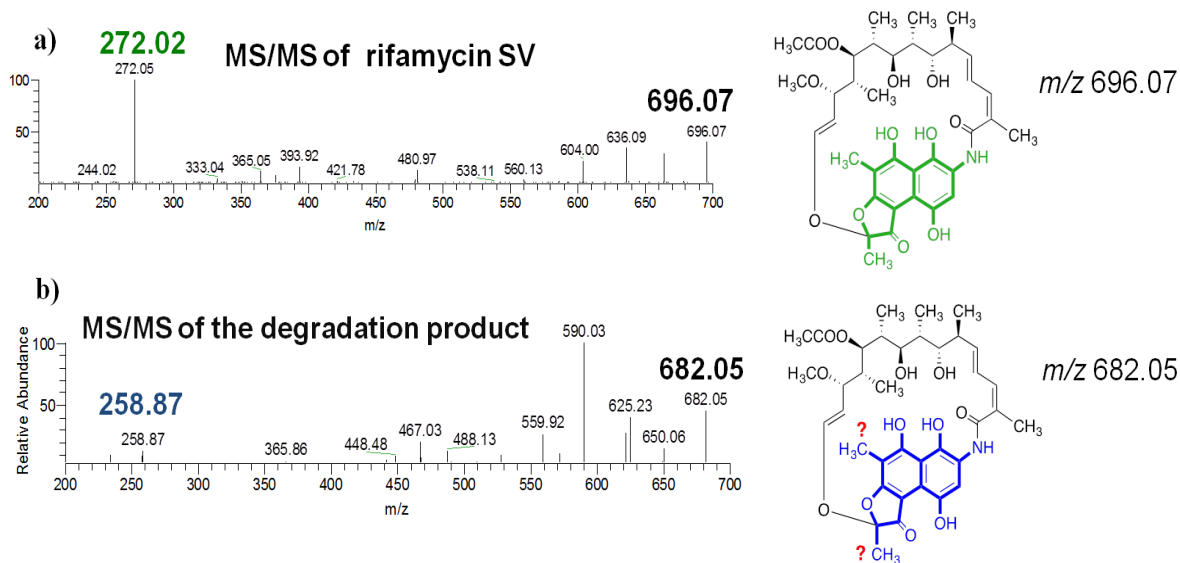

Figure 9: a) The tandem mass spectrum of rifamycin SV. b) The tandem mass spectrum of the degradation product.

While scaling up the production, the use of minimal media proved to be unable to support cellular growth and was not further pursued. The use of modified YMG media,

however, did show substantial growth after 35 days and mass spectrometry analysis revealed the production of the putative desmethylrifamycin SV product, in addition to rifamycin B (Figure 10). The peak associated with the desmethylrifamycin SV metabolite is at *m/z* 682 [M-H]⁻ whereas a peak at *m/z* 754 [M-H]⁻ represented rifamycin B.

Figure 10: LC-MS analysis of the crude extracts of A. mediterranei S699 solid cultures after 35 days. a) Analysis of the crude extract of the yeast: 2 g/L, malt extract: 5 g/L, glucose: 0 g/L plate. b) Analysis of the crude extract of the yeast: 4 g/L, malt extract: 10 g/L, glucose: 0.5 g/L plate. c) Analysis of the crude extract of the yeast: 1 g/L, malt extract: 2 g/L, glucose: 0.5 g/L plate. d) Analysis of the crude extract of the yeast: 2 g/L, malt extract: 5 g/L, glucose: 0.25 g/L plate.

28

The ratio of desmethylrifamycin SV to rifamycin B was less than optimal at 35 days of room temperature incubation. Figure 11 shows the same plates after an additional 11 days, making a total of 46 days of incubation.
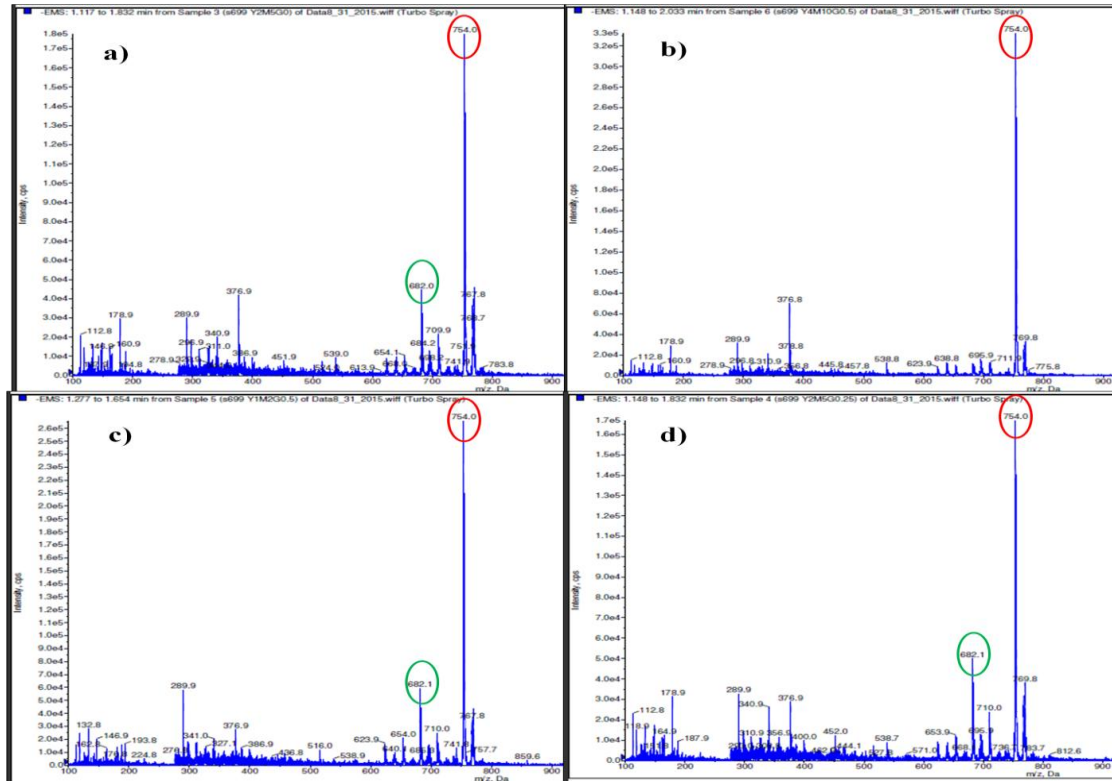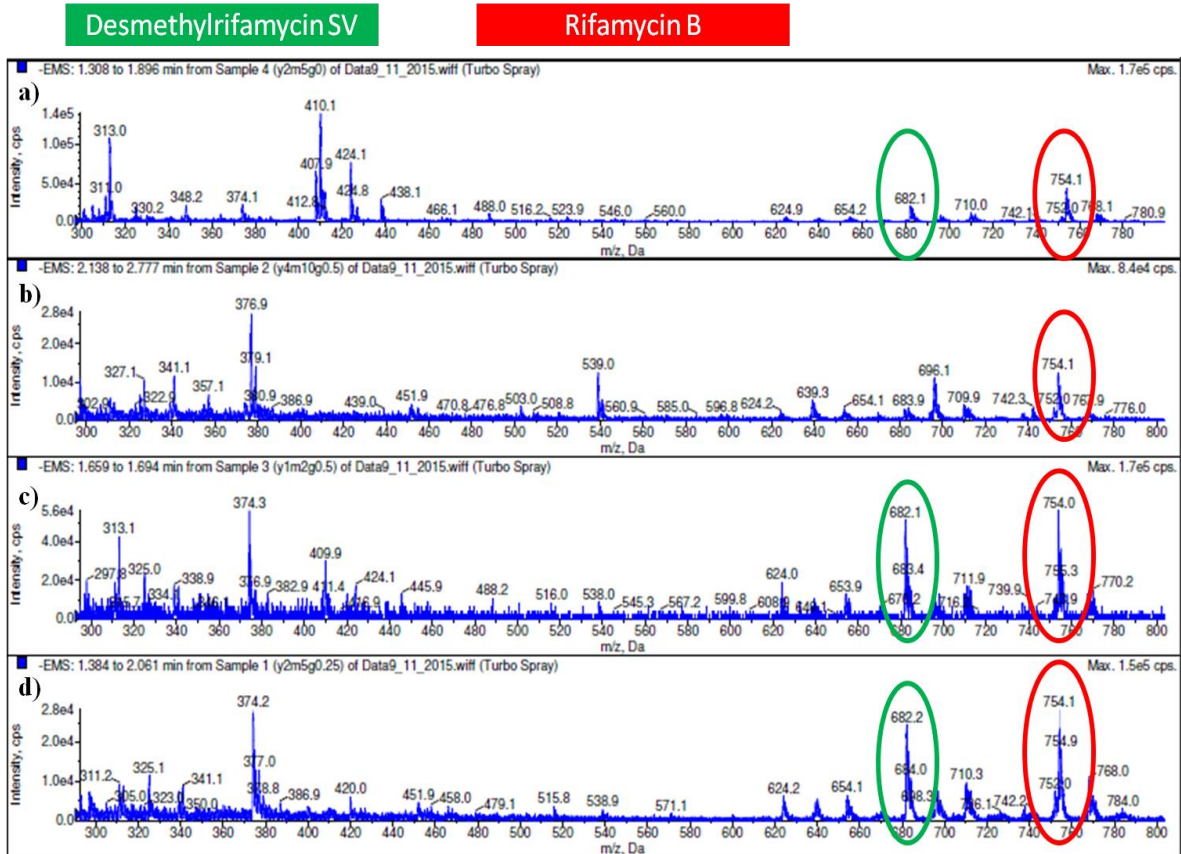

Figure 10: LC-MS analysis of the crude extract of A. mediterranei S699 solid cultures after 46 days. a) Analysis of the crude extract of the yeast: 2 g/L, malt extract: 5 g/L, glucose: 0 g/L plate. b) Analysis of the crude extract of the yeast: 4 g/L, malt extract: 10 g/L, glucose: 0.5 g/L plate. c) Analysis of the crude extract of the yeast: 1 g/L, malt extract: 2 g/L, glucose: 0.5 g/L plate. d) Analysis of the crude extract of the yeast: 2 g/L, malt extract: 5 g/L, glucose: 0.25 g/L plate.

After longer incubation, the various agar plates showed better 1:1 ratios of the metabolites, desmethylrifamycin SV and the rifamycin B. The 1:1 ratio was preferred as

it would provide significant metabolite for further testing but avoid further degradation. The plate with the YMG concentrations of yeast: 1 g/L, malt extract: 2 g/L, and glucose: 0.5 g/L (plate c in both Figure 10 and Figure 11) was selected because of the presence of the most desmethylrifamycin SV as well as the closest 1:1 ratio.

3.4.2. HPLC Purification of Desmethylrifamycin SV

The peak on Figure 12 shows that the peak retention time of the sample was roughly 8.5 minutes at a flow rate of 2 mL/min. The column in use was a YMC column, 250 x 10 mm, acetonitrile-(0.005 M) ammonium formate gradient (40 % acetonitrile for 12 min, then 100 % acetonitrile for 25 min, then 40 % for 30 min). The title compound was collected at this peak retention time and after drying measured to be 1.3 mg.
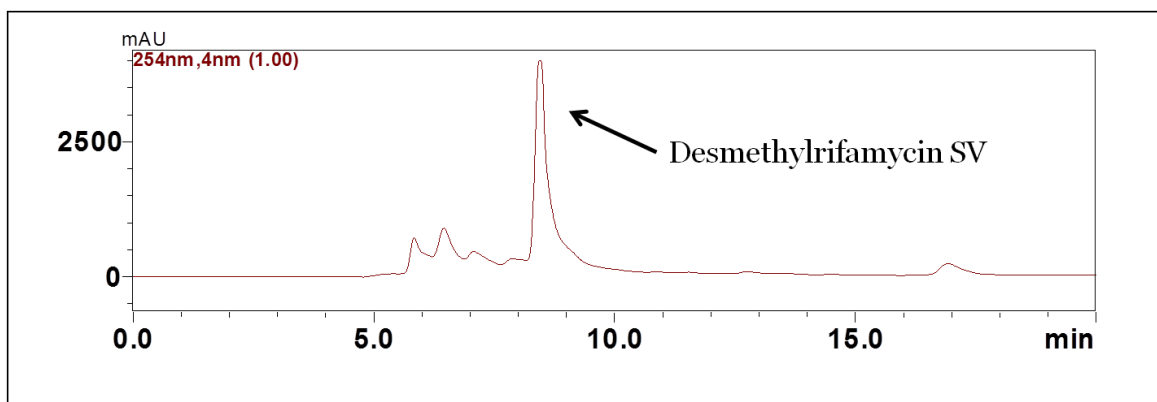
Figure 12: HPLC for 12-desmethylrifamycin SV purification.

3.4.3. ^{1}H NMR of 12-desmethylrifamycin SV

The ^{1}H NMR spectrum, performed in methanol-d4, of the isolated compound revealed that the degradation product was not the desired 7-desmethylrifamycin SV but was 12-desmethylrifamycin SV. This was confirmed by the absence of the C-12 methyl signal at 1.7 ppm and the appearance of a singlet at 6.3 ppm, which is consistent with the

presence of a proton at C-12. 12-desmethylrifamycin SV: Brownish powder, ^{1}H NMR
(500 MHz, CD$_3$OD): δ6.90 (s, 1H),), 6.40 (dd, J = 10, 5 Hz,1H), 6.31 (s, 1H), 6.31 (bd, J
= 5 Hz, 1H), 6.17 (bd, J = 5 Hz, 1H), 6.08 (dd, J = 10, 5 Hz,1H), 5.25 (m, 1H), 5.12 (d, J
= 5 Hz, 1H), 3.85 (d, J = 5 Hz, 1H), 3.34 (m, 1H), 3.07 (m, 1H), 3.07 (s, 3H), 2.35 (m,
1H), 2.17 (s, 3H), 2.06 (s, 3H), 2.01 (s, 3H), 1.83 (m, 1H), 1.67 (m, 1H), 1.48 (m, 1H),
1.04 (d, J = 5 Hz, 3H), 0.94 (d, J = 5 Hz, 3H), 0.67 (d, J = 5 Hz, 3H), 0.06 (d, J = 5 Hz,
3H). Low resolution ESI-MS m/z [M-H]$^-$: 682.71). Figure 13 shows a comparison
between ^{1}H NMR spectrum of 12-desmethylrifamycin SV (Figure 13a) and that of
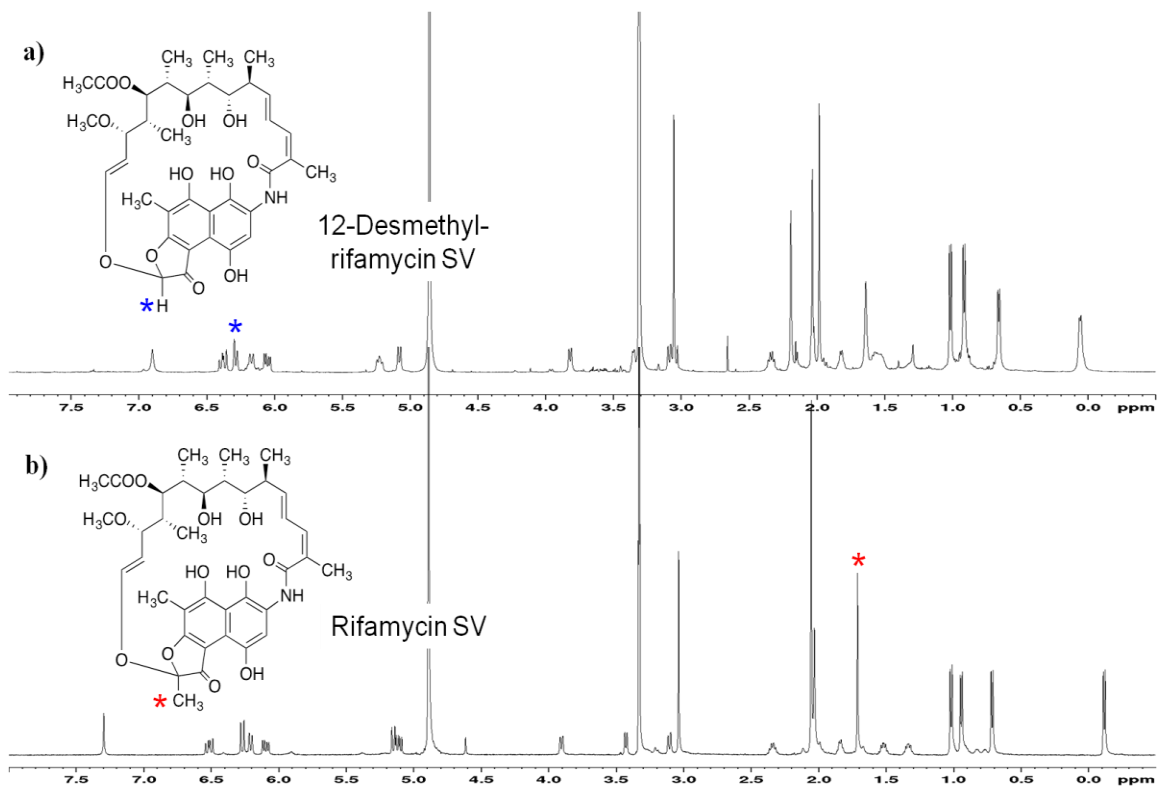rifamycin SV (Figure 13b).

Figure 13: ^{1}H NMR spectra for both a) 12-desmethylrifamycin SV and b) rifamycin SV. The lack of a singlet at a shift of 1.7 ppm indicates that there is no longer a methyl at the 12th carbon on the ring structure of the rifamycin.

3.4.4. Antibiotic Activity of 12-desmethylrifamycin SV

Although 12-desmethylrifamycin SV was not the intended compound to test the current hypothesis that a 7-desmethyl analog of rifamycin would be more effective against MDR-TB, the former compound does have potential for antibiotic properties. Therefore, 12-desmethylrifamycin SV was tested against *M. tuberculosis* H37Rv and the rpoB S531L (50_3) mutant. The results showed that the new analog had good antibacterial activity against *M. tuberculosis* H37Rv, with a minimum inhibitory concentration (MIC) comparable to that of rifamycin SV (Table 2). However, there was no significant effect against the rpoB S531L (50_3), mutant indicating that it is not effective against MDR-TB.

Table 2: Minimum inhibitory concentrations (μg/mL) of 12-desmethylrifamycin SV, rifampin, and rifamycin SV against M. tuberculosis and rpoB S531L (50_3).

Compound	Top Concentration Tested	*M. tuberculosis* H37Rv	rpoB S531L (50_3)
12-Desmethyl-rif SV	10 μg/mL	0.014	>10
Rifampin	10 μg/mL	0.004 9	>5
Rifamycin SV	25 μg/mL	<0.01 2	19

CHAPTER 4

Cloning and Expression of *rif-Orf13* and *rif-Orf16* as Putative Cytochrome P450 Enzymes Involved in the Demethylation of Rifamycin

4.1. Introduction

After the identification of 12-desmethylrifamycin it was deduced that the selective removal of the C-12 methyl group of rifamycin must take place through enzyme catalysis. As a result, a search for the enzyme in question began. Cytochrome P450s are common heme B-containing enzymes that are involved in many redox reactions and became the initial target in finding the possible enzyme responsible for the removal of the pendant C-12 methyl group.[22] *Rif-orf* genes encode many Cytochrome P450s that participate in modifying the polyketide backbone. These genes and their proteins are the target of this study as many of them have been extensively studied. Xu et al. (2005) did extensive work on many of the *Rif-orf*s that had unknown functionality.[23] Based on these findings, *rif-orf13* and *rif-orf16* were chosen as possible genes responsible for the demethylation of the polyketide backbone of rifamycin.

4.3. Experimental Section

4.3.1. Cloning of *rif-orf13* and *rif-orf16* to pRSET B

For the construction of the pTMK007 and pTMK006 plasmids for the over-expression of the *rif-orf13* and *rif-orf16* genes and Orf13 and Orf16 proteins, primers were used in the PCR reactions. For *rif-orf13*, a 1.25-kb gene, the primers were designed to have a BglII or an EcoRI restriction sites at the 5´-ends. The forward primer was 5'-GA*AGATCT*ATGACCGCCACCGCCAAGCCT-3' and the reverse primer was 5'-G*GAATTC*CCTAAGCGAGCTTCAGGG-3'. For *rif-orf16*, a 1.17-kb gene, the primers were designed to have BglII and HindIII restriction sites at the 5´-ends. The forward primer was 5'-GA*AGATCT*GTGCCGCCCGCTTTGGTGGCC-3' and the reverse primer was 5'-CCG*AAGCTT*TTAGGGAGCGTCCCAGGCGAT-3'. These fragments were obtained by PCR amplification using *A. mediterrainei* S699 chromosomal DNA as a template. The vector pRSET B was cut with both BglII and EcoR1 and BglII and HindIII for *rif-orf13* and *rif-orf16*, respectively. After digestion, the plasmids were treated with shrimp alkaline phosphatase. The plasmids and fragments were ligated, creating pTMK007 for *rif-orf13* and pTMK006 for rif-*orf16*. The plasmids were electroporated into *E. coli* DH10β cells and colonies were selected after overnight growth on antibiotic (ampicillin) selective plates. Figure 14 shows both pTMK007 and pTMK006.
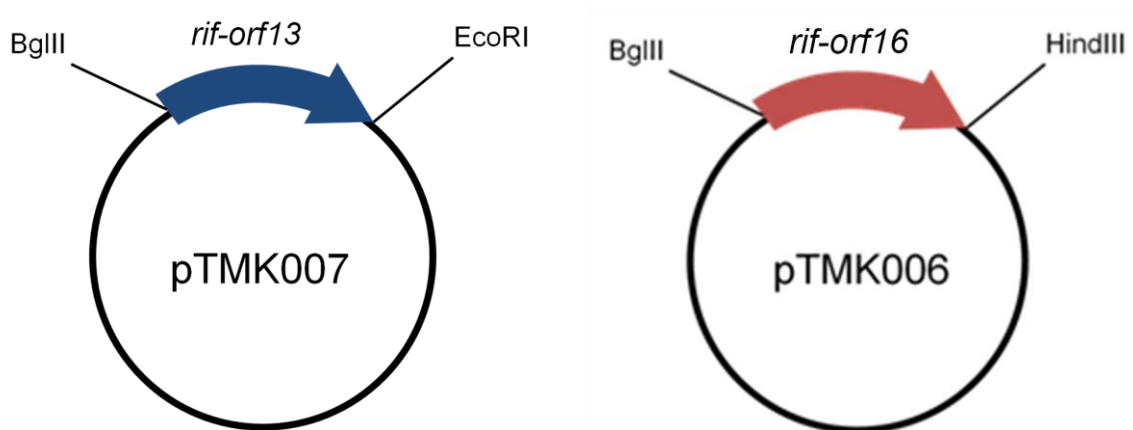
Figure 14: Vectors with rif-orf13 and rif-orf16 inserted into pRSET B.

4.3.2. Electroporation into *E. coli* BL21(DE3) pLysS Competent Cells for Protein Expression

The plasmids were isolated and then transformed, via heat shock, into chemically competent cells. *E. coli* BL21(DE3) pLysS contains the pLysS plasmid that has a chloramphenicol resistance gene as well as T7 lysozyme which lowers the background protein expression level without interfering with the level of expression achieved during the induction by IPTG. Colonies were selected from the ampicillin and chloramphenicol containing plates.

4.3.3. Protein Over-Expression

Protein expression was performed both at 18 °C and 30 °C overnight in LB for *rif-orf13*. Before overnight expression, the cultures were supplemented with (0.5 mM) δ-

amino-levulinic acid and (100 mM) IPTG. For *rif-orf16*, the protein expression was run exclusively at 18 °C but in both LB and TB media.

4.3.4. SDS-PAGE

Aliquotes of the cells after protein expression were sonicated, keeping some lysate and supernatant after centrifugation. The samples were run on an SDS-PAGE gel according to standard procedure.

4.4. Results and Discussion

4.4.1 Construction of pTMK007 and pTMK006

The construction of the final pTMK007 and pTMK006 took multiple attempts at ligation and electroporation. Insertion was confirmed using restriction enzyme digestion and gel electrophoresis. Figure 15a shows the resultant gel using a single digestion with BamHI of pTMK007. This digestion made two cuts in the plasmid, resulting in 3-kb and 1.25-kb bands. Figure 15b represents the single and double digestion of pTMK006. The single digestion was with HindIII, providing the 4.2-kb band and the double digestion used HindIII and BglII giving a 3-kb band and a 1.17-kb band. The digestions and gels did confirm that ligation was successful.
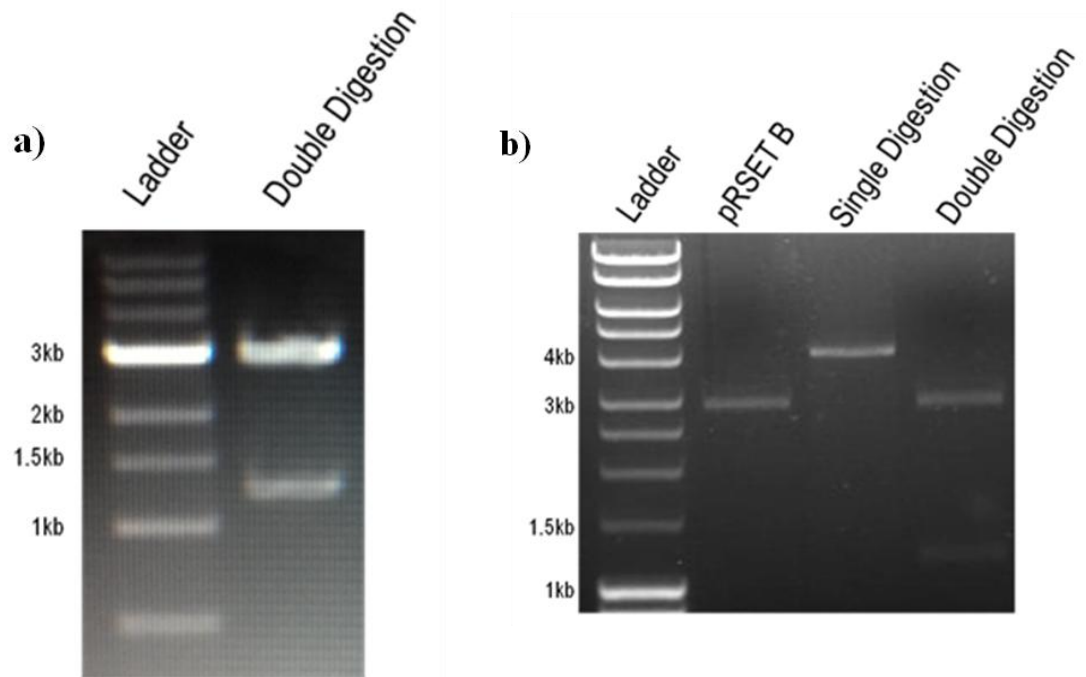
Figure 15: a) The single digestion of pTMK007 with BamH1 resulting in two bands at 3-kb and 1.2-kb. b) The single and double digestion of pTMK006. The single digestion was with HindIII producing a 4.2-kb band and the double digestion was with HindIII and BglII producing a 3-kb band and a 1.17-kb band.

4.4.2. SDS-PAGE Analysis

The SDS-PAGE gels were ran separately for Orf13 and Orf16. The Orf13 gel is shown in Figure 16. As can be seen in the image, protein over-expression is observed in both the 18 °C and 30 °C overnight temperature experiments at the expected 47 kDa molecular weight. There does seem to be more expression in the 18 °C lysate. Based on the lack of over-expression in the soluble protein, Orf13 is not soluble under the current conditions and more solubility trials will be necessary.
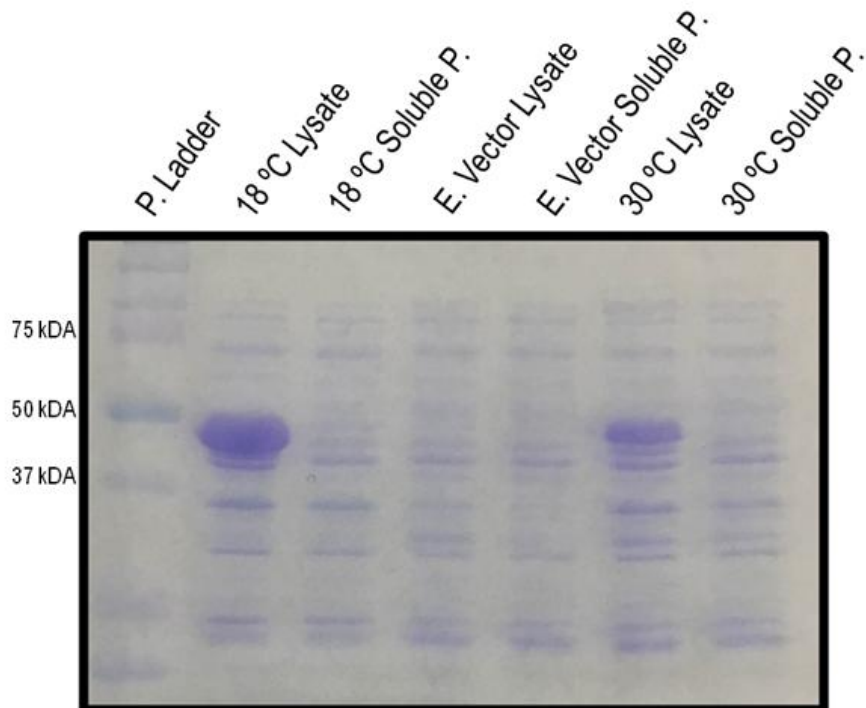
Figure 16: SDS-PAGE gel for Orf13 at both 18 °C and 30 °C. The empty vector was used for comparison purposes to determine over-expression. Over-expression can be seen at the expected 47 kDa.

Figure 17 shows the resultant SDS-PAGE gel for Orf16, testing both LB and TB medias to explore solubility of the protein. As can be seen by the gel, over-expression did occur based on the presence of a large band at 43 kDa, the expected molecular weight. However, there is again, no protein in the soluble protein lanes, indicating that again, the protein is not soluble in the media used. Further experimentation is necessary to troubleshoot this issue.
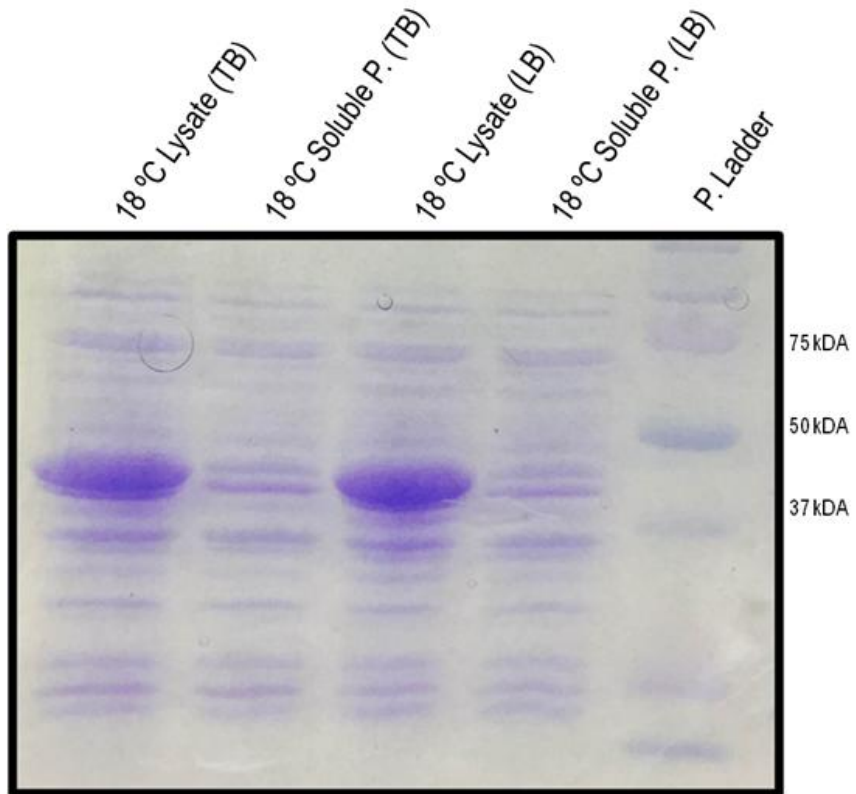
Figure 17: SDS-PAGE gel for Orf16 in both LB and TB media. Over-expression can be seen at the expected 43 kDa.

CHAPTER 5

CONCLUSION

Tuberculosis is a dangerous and highly contagious disease that is all too common in highly populated and underdeveloped nations. The overuse and misuse of antibiotics has lead to a new crisis in TB treatment, multidrug resistant TB. These strains of *Mycobacterium tuberculosis* have mutated their RNA polymerase, the target of rifampin, so as to not allow inhibition. This led to the investigation of a new analog of rifamycin B, the precursor to rifampin, to target such mutated RNA polymerase. Through a separate bio-computational study, 7-desmethylrifamycin (shown in Figure 18) was determined to be a promising target molecule. Starting with the double crossover recombination experiments outlined in chapter 2, there was difficulty associated with the transformation of the replacement cassette into the *A. mediterranei* competent cells. After this difficulty persisted, another tactic was approached using product degradation via cell starvation. It was noticed that when plates of *A. mediterranei* were allowed to sit at room temperature for an extended period of time, a metabolite with the same mass as a desmethylrifamycin SV began to appear in mass spectrometry. This molecule was later determined to be 12-desmethylrifamycin SV (shown in Figure 18). Although this molecule did not show antibiotic activity against MDR-TB, it did show significant activity against non-resistant tuberculosis. Based on an assumption that the degradation of the rifamycin B to 12-desmethylrifamycin SV was due to an enzyme, the next approach centered on determining the enzyme responsible. Two proteins were chosen for investigation, Orf13 and Orf16, based on their proximity to the biosynthetic gene cluster and their unknown

function. These genes were cloned and heterologously expressed in *E. coli*. However, the recombinant proteins were insoluble. The insolubility of the protein posed some problems for testing, as purified proteins are preferred for further testing for functionality. Further exploratory work is necessary to find a proper condition, under which Orf13 and Orf16 can be produced in their soluble forms. Future work will include the characterization of Orf13 and Orf16 and their role in the production of 12-desmethylrifamycin SV, as well as exploration of alternative approaches to produce 7-desmethylrifamycin, which is predicted to be active against MDR-TB.
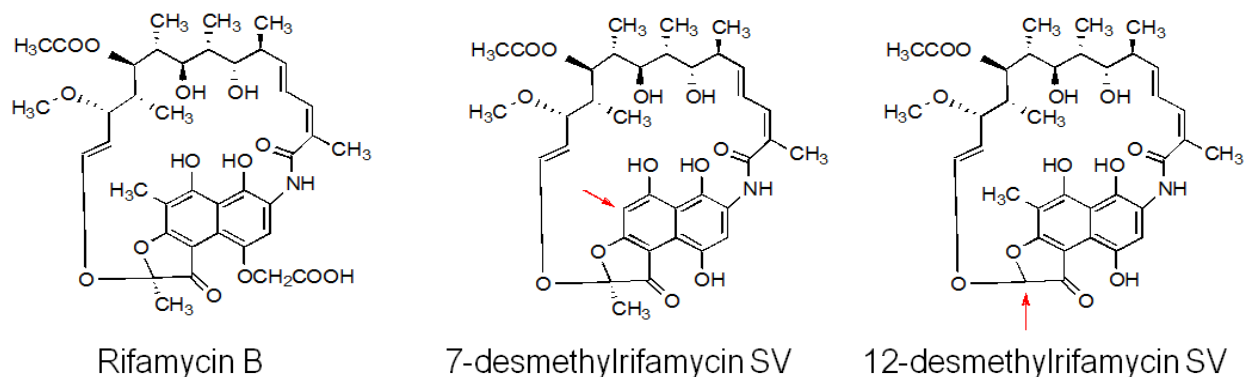

Figure 18: A comparison between the structures of rifamycin B, 7-desmethylrifamycin SV, and 12-desmethylrifamycin SV.

REFERENCES

[1] Daniel, TM., The history of tuberculosis. *Respir Med* **2006**, 100(1), 1862-70.

[2] Rutgers Global Tuberculosis Institute, History of Tuberculosis. http://globaltb.njms.rutgers.edu/abouttb/historyoftb.html

[3] Thayer A., Taking Down TB. *Chemical and Engineering News* **2007**, 85(39), 21-32.

[4] Center for Disease Control and Prevention. Multidrug-Resistant Tuberculosis (MDR TB). **2016.** http://www.cdc.gov/tb/publications/factsheets/drtb/mdrtb.htm

[5] World Health Organization Global Report 2016. http://www.who.int/tb/global-tb-report-infographic.pdf?ua=1

[6] World Health Organization. Tuberculosis: Fact Sheet. **2016**. http://www.who.int/mediacentre/factsheets/fs104/en/

[7] Rajeswari, R.; Balasubramanian, R.; Muniyandi, M.; Geetharamani, S.; Thresa, X.; Venkatesan, P., Socio-economic impact of tuberculosis on patients and family in India. *Int J Tuberc Lung Dis* **1999**, 3(10), 869-877.

[8] Kim J.Y., Shakow A., Castro A., Vande C., Farmer P., Tuberculosis control. World Health Organization. http://www.who.int/trade/distance_learning/gpgh/gpgh3/en/index1.html

[9] Morris M.D.; Quezada L.; Bhat P.; Moser K.; Smith J.; Perez H.; Laniado-Laborin R.; Estrada-Guzman J.; Rodwell T.C., Social, Economic, and Psychological Impacts of MDR-TB Treatment in Tijuana, Mexico: A Patient's Perspective. *Int J Tuberc Lung Dis* **2014**, 17 (7), 954-960.

[10] Ananthakrishnan R.; Jeyaraj A.; Palani G.; Sathiyasekaran B.W.C., Socioeconomic impact of TB on patients registered with RNTCP and their families in the year 2007 in Chennai, India. *Lung India* **2012**, 29(3), 221-226.

[11] ZaffiriL.; Gardner J.; Toledo-Pereyra L.H., History of antibiotics. From Salvarsan to cephalosporins. *J Invest Surg* **2012**, 25(2), 67-77.

[12] Aminov R.I., A Brief History of the Antibiotic Era: Lessons Learned and Challenges for the Future. *Front Microbiol* **2010**, 1, 1-7.

[13] Sensi, P., History of the Development of Rifampin. *Clin Infect Dis* **1983** 5, 402-406.

[14] Center for Disease Control and Prevention. Treatment for TB Disease. http://www.cdc.gov/tb/topic/treatment/tbdisease.htm

[15] Jnawali H.N.; Ryoo S., **2013**. First– and Second–Line Drugs and Drug Resistance, Tuberculosis - Current Issues in Diagnosis and Management, Dr. Bassam Mahboub (Ed.), InTech, DOI: 10.5772/54960. http://www.intechopen.com/books/tuberculosis-current-issues-in-diagnosis-and-management/first-and-second-line-drugs-and-drug-resistance

[16] Floss H.G.; Yu T., Rifamycin—Mode of Action, Resistance, and Biosynthesis. *Chem Rev* **2005** 105 (2) 621-632.

[17] Campbell E.A.; Korzheva N.; Mustaev A.; Murakami K.; Nair S.; Goldfarb A.; Darst S., Structural Mechanism of Rifampicin Inhibition of Bacterial RNA Polymerase. *Cell* **2001**, 104 (6) 901-912.

[18] Somoskovi A.; Parsons L.M.; Salfinger M., The molecular basis of resistance to isoniazid, rifampin, and pyrazinamide in Mycobacterium tuberculosis. *Respiratory Research* **2001**, 2(3), 164-168.

[19] Nigam A.; Almabruk K.H.; Saxena A.; Yang J.; Mukherjee U.; Kaur H.; Kohli P.; Kumari R.; Singh P.; Zakharov L.N.; Singh Y.; Mahmud T.; Lal R., Modification of Rifamycin Polyketide Backbone Leads to Imporved Drug Activity against Rifampicin-resistant Mycobacterium tuberculosis. *Journal of Biological Chemistry* **2014**, 289(30), 21142-21152.

[20] Lal, R.; Khanna R.; Dhingra N.; Khanna M.; Lal S., Development of an imporved cloning vector and transformation in Amycolatopsis mediterranei (Nocardia mediterranei). *J Antibiot (Tokyo)* **1998**, 51(2), 161-169.

[21] Xu J.; Mahmud T.; Floss H.G., Isolation and characterization of 27-O-demethylrifamycin SV methyltrasnferase provides new insights into the post-PKS modification steps during the biosynthesis of the antitubercular drug rifamycin B by Amycolatopsis mediterranei S699. Archives of Biochemistry and Biophysics 2003 411(2), 277-288.

[22] Munro A.W.; Girvan H.M.; McLean K.J., Cytochrome P450-redox partner fusion enzymes. *Biochimica et Biophysica Acta* **2006**, 1770(3), 345-359.

[23] Xu J.; Wan E.; Kim C.; Floss H.G.; Mahmud T., Identification of tailoring genes involved in the modification of the polyketide backbone of rifamycin B by Amycolatopsis mediterranei S699. *Microbiology* **2005** 151(8), 2515-2528.